ACS APPLIED MATERIALS & INTERFACES

Research Article

www.acsami.org

Sub-100 nm Gold Nanoparticle Vesicles as a Drug Delivery Carrier enabling Rapid Drug Release upon Light Irradiation

Kenichi Niikura,*[,†,§] Naoki Iyo,[‡] Yasutaka Matsuo,[†,§] Hideyuki Mitomo,[†,§] and Kuniharu Ijiro[†,§]

[†]Research Institute for Electronic Science (RIES), Hokkaido University, Kita 21, Nishi 10, Kita-Ku, Sapporo 001-0021, Japan

[§]JST-CREST, Sanban-cho 5, Chiyoda-ku, Tokyo 102-0075, Japan

[‡]Graduate School of Chemical Science and Engineering, Hokkaido University, Kita13, Nishi8, Kita-Ku, Sapporo 060-8628, Japan

Supporting Information

ABSTRACT: Previously, we reported gold nanoparticles coated with semi-fluorinated ligands self-assembled into gold nanoparticle vesicles (AuNVs) with a sub-100 nm diameter in tetrahydrofuran (THF).[1] Although this size is potentially useful for in vivo use, the biomedical applications of AuNVs were limited, as the vesicular structure collapsed in water. In this paper, we demonstrate that the AuNVs can be dispersed in water by cross-linking each gold nanoparticle with thiol-terminated PEG so that the cross-linked vesicles can work as a drug delivery carrier enabling light-triggered release. Rhodamine dyes or anticancer drugs were encapsulated within the cross-linked vesicles by heating to 62.5 °C. At this temperature, the gaps between nanoparticles open, as confirmed by a blue shift in the plasmon peak and the more efficient encapsulation than that observed at room temperature. The cross-linked AuNVs released encapsulated drugs upon short-term laser irradiation (5 min, 532 nm) by again opening the nanogaps between each nanoparticle in the vesicle. On the contrary, when heating the solution to 70 °C, the release speed of encapsulated dyes was much lower (more than 2 h) than that triggered by laser irradiation, indicating that cross-linked AuNVs are highly responsive to light. The vesicles were efficiently internalized into cells compared to discrete gold nanoparticles and released anticancer drugs upon laser irradiation in cells. These results indicate that cross-linked AuNVs, sub-100 nm in size, could be a new type of light-responsive drug delivery carrier applicable to the biomedical field.

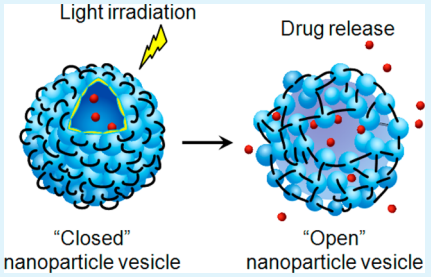

KEYWORDS: *gold nanoparticles, capsules, vesicles, drug delivery, light-triggered release*

1. INTRODUCTION

Micro- and nanocapsules have structures that enable them to be used in wide range of applications, including microreactors and drug delivery systems.[2] The self-assembly of lipids, polymers, and proteins has been used for the formation of micro- or nanocapsules such as liposomes,[3,4] polymeric capsules,[5−7] and virus-like particles.[8,9] As a drug delivery carrier, capsules provide important functions in terms of controlled release, protection from degradation in the body and high-level of drug loading without chemical modification.[2] In addition, there are two critical properties necessary for a drug delivery carrier, particularly for tumor targeting: a suitably sized carrier and the controlled release of the loaded drugs.[10] A diameter of between 10 and 200 nm allows long-term circulation[11] and tumor targeting[12] in vivo. Localized drug release on external stimulus reduces the likelihood of adverse effects.

As gold nanostructures, such as gold nanoparticle (AuNP) and nanorod, can interact with external light,[13−18] gold-nanostructure-containing capsules afford a promising light-responsive drug carrier. To date, the light-triggered release of encapsulated molecules from AuNP-embedded liposomes,[19] or polyelectrolytes,[20,21] mesoporous silica-coated gold nanorods,[22,23] and gold nanoshell−hydrogel conjugates[24] have been reported. However, in general, in the previous systems, the release speed of drugs is relatively low (several hours) and/or the capsules are too large for biomedical applications. For light-triggered release, high responsiveness to light stimulus is vitally important for the specific and efficient delivery of drugs to target sites in vivo.

Recently, the approaches to assembling of various kinds of nanoparticles to 2D or 3D structure have been developed toward the electronic and bioapplications.[25,26] For example, the vesicular assembly of nanoparticles (referred to as nanoparticle vesicles; NVs), which assume a hollow structure with a nanoparticle shell, have been reported as a new type of capsule.[27−33] In particular, the response of the gold nanoparticle vesicles (AuNVs) to light irradiation is expected to be more sensitive than that of single nanoparticle systems due to the high AuNP content. In fact, the increase in the gold content in the lipid bilayer of the liposome improves the response to light irradiation.[34] Xia et al. successfully demonstrated that gold nanocages covered with a thermally responsive polymer, Poly(N-isopropylacrylamide), could release anticancer drugs

Received: February 15, 2013
Accepted: April 8, 2013
Published: April 8, 2013

upon laser irradiation.[35] Therefore, the AuNVs could act as a highly light-responsive drug carrier.

Rotello et al.[36] and Duan et al.[37] reported that AuNVs could encapsulate anticancer drugs and act as a drug delivery carrier, respectively. However, the light-responsive property of the AuNVs has not yet been utilized for release of the encapsulated drug molecules. In the only report of light-triggered dye release from nanoparticle vesicles identified in our search of the literature, relatively large vesicles (with a diameter of ca. 500 nm) were used and the dyes were gradually released during irradiation (~40 min).[38,39] Recently, we reported that gold nanoparticles coated with semifluorinated surface ligands (SFL) self-assembled in THF to provide AuNVs with a diameter of sub-100 nm,[1] in which the assembly of fluorinated segments was considered to contribute to the vesicular assembly of the nanoparticles.[40−42] The AuNVs were well-dispersed in organic solvents, such as chloroform; however, the vesicular structure was unstable in water, limiting biomedical applications.

In this paper, we report that our new water-dispersible AuNVs, small enough for in vivo use, could encapsulate drugs and rapidly release them upon light irradiation. To our knowledge, this is the first report to demonstrate that AuNVs can act as a light-sensitive drug carrier into cells. The cross-linking of each nanoparticle within a vesicle by thiol-terminated poly(ethylene glycol) (dithiol-PEG) made the AuNVs water-dispersible (Scheme 1) and their hollow structure remained stable even in water. We found that dyes or drugs could enter the cross-linked AuNVs through the interparticle gaps at high temperature and were encapsulated inside the vesicles due to the closure of these gaps at room temperature. Furthermore, they were released from cross-linked AuNVs by light-irradiation much more quickly (within 5 min) than in systems using solvent heating. This highly light-responsive release is probably due to the rapid motion of the AuNPs in opening of the interparticle gaps in the cross-linked AuNVs.

Scheme 1. Fabrication of Gold Nanoparticle Vesicles (AuNVs) Encapsulating Dye or Drug Molecules and Their Light-Triggered Release: (a) Surface Modification of Gold Nanoparticles (AuNPs) with Semi-fluorinated Ligands (SFL); (b) Self-Assembly of SFL-AuNPs to AuNV Formation; (c) Cross-linking of AuNPs of the AuNVs with Dithiol-PEG in THF and the Cross-Linked AuNVs Dispersed in Water; (d) Encapsulation of Dye or Drug Molecules at 62.5 °C, and Subsequent Cooling down to Room Temperaturel (e) Dye Release through Opened Interparticle Nanogaps Induced by Laser Irradiation

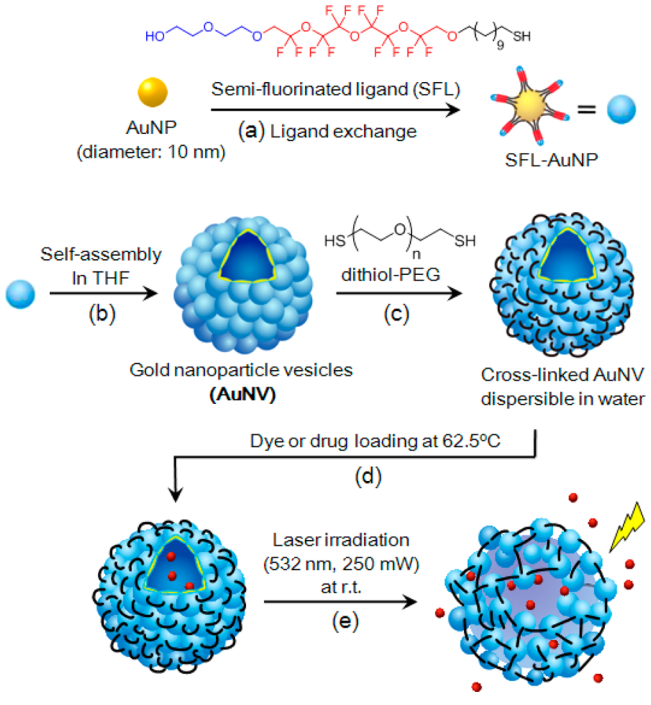

2. EXPERIMENTAL SECTION

2.1. Materials and Instruments. All commercially available reagents were used without further purification. All solvents were purchased from Wako Pure Chemical Industries Ltd. (Japan) and used without further purification. AuNPs in aqueous solution (10 nm in diameter) were purchased from British Biocell International, Ltd. (Britain). AuNPs were concentrated with a CF-16RX centrifuge (Hitachi-Koki, Ltd., Japan). Scanning Transmission Electron Microscope (STEM) images were obtained using a STEM HD-2000 system (Hitachi High-Tech Manufacturing & Service Co., Ltd., Japan) with an accelerating voltage of 200 kV. UV−vis spectra were measured with a UV−vis spectrophotometer UV-1650PC (Shimadzu Corporation, Japan). DLS analysis was measured with a Delsa Nano HC system (Beckman Coulter, Inc., Japan). Fluorescence from the dye molecules were was measured with a RF-5300PC fluorescence spectrometer (Shimadzu Corporation, Japan). A diode-pumped solid-state laser (CW laser, 532 nm, Millenia X, Spectra-Physics, Japan) was used for light-triggered release of dye molecules and DOX. Inductively coupled plasma emission spectrometry (ICPES) was performed using an ICPE-9000 system (Shimadzu Corporation, Japan). The numbers of cells were counted using a Scepter hand-held automated cell counter (Millipore Corporation, USA). The ratio of dead cells was obtained from cell images captured using an IX70 inverted microscope (Olympus Corporation, Japan).

2.2. Synthesis of Semi-fluorinated Ligand (SFL). SFL was synthesized as described in our previous literature[1] and stored as a 40 mM methanol solution at 4 °C.

2.3. Preparation and Interparticle Cross-Linking of AuNVs. The aqueous dispersions of citrate-stabilized AuNPs (500 μL, 9 nM, 10 nm in diameter) were concentrated by centrifugation (10,000 rpm, 4 °C, 40 min) and then added into a THF solution (500 μL) of SFL (0.2 mM), followed by vigorous stirring overnight. We note that the concentration of thiols in this solution was 7.5 times that of total Au atoms on the nanoparticle surface. The resulting solutions were centrifuged twice to remove the citrate and excess SFL. Dithiol-PEG (500 μL, 1 mM) in THF were added to AuNVs then incubated for 15 h. After purification by several centrifugations, AuNVs were dispersed in water. AuNVs were characterized by STEM, DLS, and absorption spectra.

2.4. Preparation of Dispersed AuNPs Modified with Dithiol-PEG. Aqueous dispersions of citrate-stabilized AuNPs (500 μL, 9 nM, 10 nm in diameter) were concentrated by centrifugation (10,000 rpm, 4 °C, 40 min) and then added into a methanol solution (500 μL) of SFL (0.2 mM), followed by vigorous stirring overnight. The resulting solutions were centrifuged twice to remove the citrate and excess SFL. Dithiol-PEG (500 μL, 1 mM) in methanol was added to the AuNPs and then incubated for 15 h. After purification by several centrifugations, AuNPs were dispersed in water.

2.5. Loading Dye Molecules into Cross-Linked AuNVs. An aqueous solution of cross-linked AuNVs (9 nM based on single particles) was mixed with Rhodamine B (10 μM as a final concentration) then incubated for 7 h at 62.5 °C. The solution was dialyzed against deionized water for 15 h at room temperature to remove free dye molecules.

2.6. Dye Release from Cross-Linked AuNVs by Heating Solution or Photothermal Conversion. a Solution of Cross-Linked AunVs containing Rhodamine B was heated to 70 °C or irradiated by CW laser (532 nm, 250 or 25 mW) or Tsunami Ti:sapphire lasers (Spectra Physics, 790 nm, 250 mW). After respective incubation, the

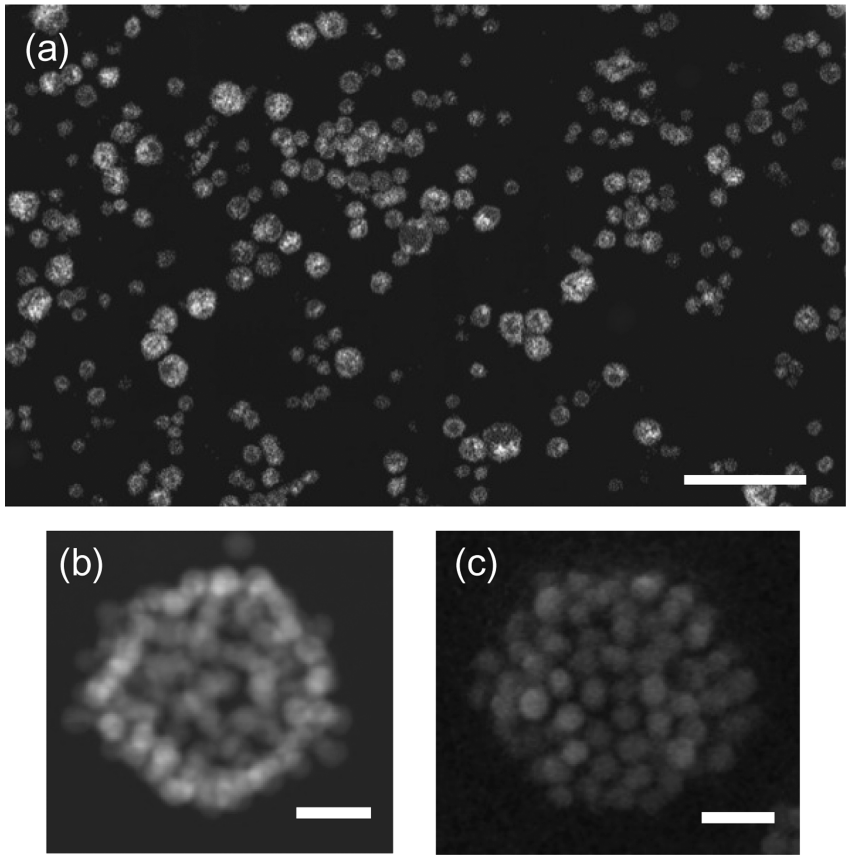

Figure 1. (a) STEM image of AuNVs cross-linked with dithiol-PEG (M_n = 3400) cast from water. (b) STEM and (C) SEM images of a single cross-linked AuNV. The scale bars are (a) 400 and (b,c) 20 nm.

cross-linked AuNVs were precipitated by centrifugation to decant the supernatant containing dye molecules released from AuNVs to a quartz cell for fluorescence measurement. The number of dye molecules released from AuNVs was calculated from fluorescence intensity (Exciation: 550 nm).

2.7. Cell Culture. HeLa cells (6,000 cells for drug release experiment, or 100,000 cells for ICPES analysis) were seeded onto a 96-well microplate and grown in Dulbecco's modified essential medium (DMEM) supplemented with 10% fetal bovine serum (FBS) and 1% antibiotics (penicillin/streptomycin) in 5% CO_2 at 37 °C for 24 h.

2.8. Determination of the Level of Cellular Uptake of Cross-Linked AuNVs by ICPES. A solution of cross-linked AuNVs or dispersed AuNPs in HEPES buffer (200 μL, 90 nM based on single particles) was mixed with Opti-MEM (2 mL), and the mixture was added to the wells of a 6-well plate followed by incubation for 2 h. After rinsing three times with PBS, the cells were trypsinized with 500 μL of trypsin/EDTA for 5 min and the number of cells was counted. Cells were precipitated by centrifugation and the supernatant was removed. Cells and nanoparticles were dissolved with 1 mL of aqua regia. After incubation for 1h, the solution was diluted with 6 mL of deionized water, and the concentration of Au atoms in the solution was measured by ICPES.

2.9. Loading DOX into Cross-Linked AuNVs. An aqueous solution of cross-linked AuNVs (90 nM based on single particles) was mixed with doxorubicin (100 μM as a final concentration) then incubated for 7 h at 62.5 °C. The solution was dialyzed against a 20 mM HEPES buffer (pH 7.4) for 15 h at room temperature to remove free DOX.

2.10. Cellular Uptake of Cross-Linked AuNVs and Drug Release Induced by Laser Irradiation. The solution of cross-linked AuNVs containing DOX in HEPES buffer (10 μL) was mixed with Opti-MEM (100 μL), and the mixture was added to the 96-well microplate and the cells were incubated for 2 h. After rinsing three times with PBS, the cells were irradiated by CW laser (532 nm, 250 mW) in DMEM for 5 min. After incubation for 2 h, cells were stained with 0.4% trypan blue and the ratio of dead cells was calculated by counting the stained cells (dead cell) and unstained cells (living cells) with an optical microscope.

3. RESULTS AND DISCUSSION

AuNVs were prepared by ligand modification of AuNPs with SFL in THF according to our previous report.[1] Briefly, SFL in THF (0.2 mM, 500 μL) were added to an aqueous solution (10 μL) of citric acid-modified AuNPs (10 nm in diameter, 10 nM) to generate AuNVs. For cross-linking, after removing excess SFL by centrifugation, dithiol-PEG (M_n = 3400: ca. 23 nm in a straight conformation) in THF (1m M) was added to the AuNV solution (10 nM based on single nanoparticles) and the mixture was incubated for 3 h (Scheme 1). After centrifugation to remove excess PEGs, cross-linked AuNVs were well-dispersed in water and retained their hollow structure (Figure 1). STEM images of cross-linked AuNVs showed a high contrast between the shell and the interior indicating their characteristic hollow structure (Figure 1b). Free SFL molecules are highly soluble in THF (see Figure S1 in the Supporting Information: NMR spectra in THF-d_8); therefore, the exchange reaction with dithiol-PEGs could proceed by removing SFLs from the surface of AuNPs. The display of thiol ligands on the AuNPs can be analyzed by MALDI-TOF mass spectrometry.[43] The MALDI-TOF mass of cross-linked AuNVs provided a peak that corresponded to SFLs (see Figure S2 in the Supporting Information), indicating that SFLs remained on the AuNVs after the exchange reaction with dithiol-PEGs.

On the contrary, AuNVs without cross-linking could not maintain their capsule structure in water and the structures were collapsed (see Figure S3 in the Supporting Information). Size distribution of cross-linked AuNVs obtained from STEM images and dynamic light scatterings (DLS) clearly showed the size of sub-100 nm (Figure 2). STEM images of AuNVs before and after cross-linking with dithiol-PEGs showed an almost equivalent size distribution (Figure 2a). This data indicated that modification of dithiol-PEG on the surface of AuNVs did not affect the morphology of AuNVs. DLS indicated a small increase in size after the cross-linking of the AuNVs, proving that a dithiol-PEG layer covered the AuNVs (Figure 2b). When AuNVs were incubated with monothiol-PEG (M_n = 5000: ca. 34 nm in a straight conformation), whose one terminal is capped with a thiol group, the AuNVs appeared to be dispersed in water; however, STEM observations revealed that the structure was partially collapsed (see Figure S3 in the Supporting Information). The treatment of AuNPs with short dithiol-PEG (M_n = 1500: ca. 10 nm in a straight conformation) resulted in collapsed vesicles, which indicates that PEG of a certain length is needed for the cross-linking of each Au nanoparticle (see Figure S4 in the Supporting Information).

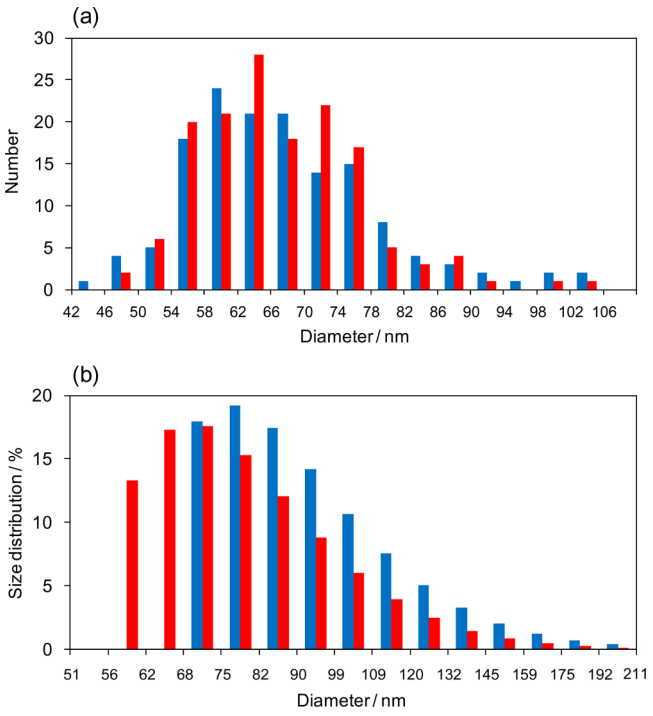

Figure 2. (a) Size distribution of AuNVs before (red bar) and after (blue bar) cross-linking with dithiol-PEG (M_n = 3400) obtained from STEM images. The counting number is 150. The average size of AuNVs vesicles were 63.6 ± 11.1 nm (before cross-linking), and 64.9 ± 14.0 nm (after cross-linking), respectively. (b) Size distribution of AuNVs before (red bar), and after (blue bar) cross-linking with dithiol-PEG obtained from DLS. The average size of AuNVs were 70.9 ± 20.1 nm (before cross-linking), and 90.7 ± 24.4 nm (after cross-linking), respectively.

Absorption spectra of cross-linked AuNV solutions at various temperatures were measured to estimate the temperature-dependent interparticle distance between each AuNP in the AuNVs. Cross-linked AuNVs with dithiol-PEG exhibited a plasmon peak at 541 nm (Figure 3a, blue line). This peak was red-shifted by about 20 nm compared to that of the monodispersed Au nanoparticles (λ_{max} = 520 nm). The plasmon peak was not shifted until the temperature was increased to 60 °C. Thereafter, a large, steep blue shift of more than 10 nm was observed during heating from 60 to 75 °C, which indicates that the interparticle nanogaps of the cross-linked AuNVs were increased (Figure 3b, blue diamonds). At high temperature,s in addition to the increased Brownian motion of AuNPs, a change in the PEG conformation (from gauche to anti) is speculated to assist in the widening of the nanogaps.[44] Oligo(ethylene oxides)-grafted polymers generally display a lower critical solution temperature (LCST).[45] The hydration change at the LCST for the AuNVs is speculated to assist in inducing the obvious change in the plasmon peak at 60−75 °C.

El-Sayed and co-workers determined the relationship between plasmon shift and interparticle distance using a discrete dipole approximation (DDA) method.[46] On the basis of their simulation results for a trimer of AuNPs (10 nm in diameter), it was estimated that the interparticle nanogap was increased from 2.5 to 4.0 nm during heating. STEM images taken before and after heating show obvious expansion of the nanogap, thus supporting our assumption (Figure 3c, d). In addition, the hydrodynamic diameter of AuNVs increased from 89.9 to 100.5 nm after incubation at 70 °C (see Table S1 in the Supporting Information), supporting the results observed in the STEM images. In the case of monothiol-PEG-modified AuNVs, a plasmon peak of 526 nm (a shift of only 6 nm compared to that of the monodispersed Au nanoparticles) was observed at 30 °C (Figure 3a, red line), indicating a wider interparticle nanogap than those of cross-linked AuNVs. When the temperature of the solution was increased to 75 °C, only a gradual, small shift in the plasmon peak was observed (Figure 3b, red diamonds). STEM images revealed that the monothiol-PEG-coated AuNVs were completely collapsed to monodispersed nanoparticles after heating the solution to 75 °C (Figure 3e, f). These data support the notion that PEG cross-linked AuNVs form a robust structure (referred as a "closed form") at the less than 60 °C and that the interparticle nanogaps widen at higher temperatures to produce an "open form".

Next, we tested Rhodamine B dye encapsulation as a drug model in cross-linked AuNVs as well as its release utilizing the temperature-dependent change in structure from the closed to open form. The mixture of Rhodamine B with cross-linked AuNVs was heated to 62.5 °C to open the interparticle gap and promote dye loading. We found that the incubation temperature of the cross-linked AuNV solution is an important factor for efficient encapsulation. The level of dye encapsulation at 62.5 °C after 7 h incubation was 3 times higher than that at room temperature (see Figure S6 in the Supporting Information). This means that the interparticle gaps widened at 62.5 °C, which is the temperature at which the gaps start to open and the gaps subsequently closed during the cooling process. After heating the solution of AuNVs at 62.5 °C, the gap between the AuNPs were considered to be irreversibly widened as the plasmon peak did not return to its original 541 nm on cooling; however, the cross-linked PEGs are thought to prevent the release of encapsulated dyes from the vesicles at room temperature.

After cooling at room temperature, free dye molecules were removed by dialysis overnight. The amount of release upon heating was measured by detection of the fluorescence from dye molecules in the supernatant after centrifugation to remove

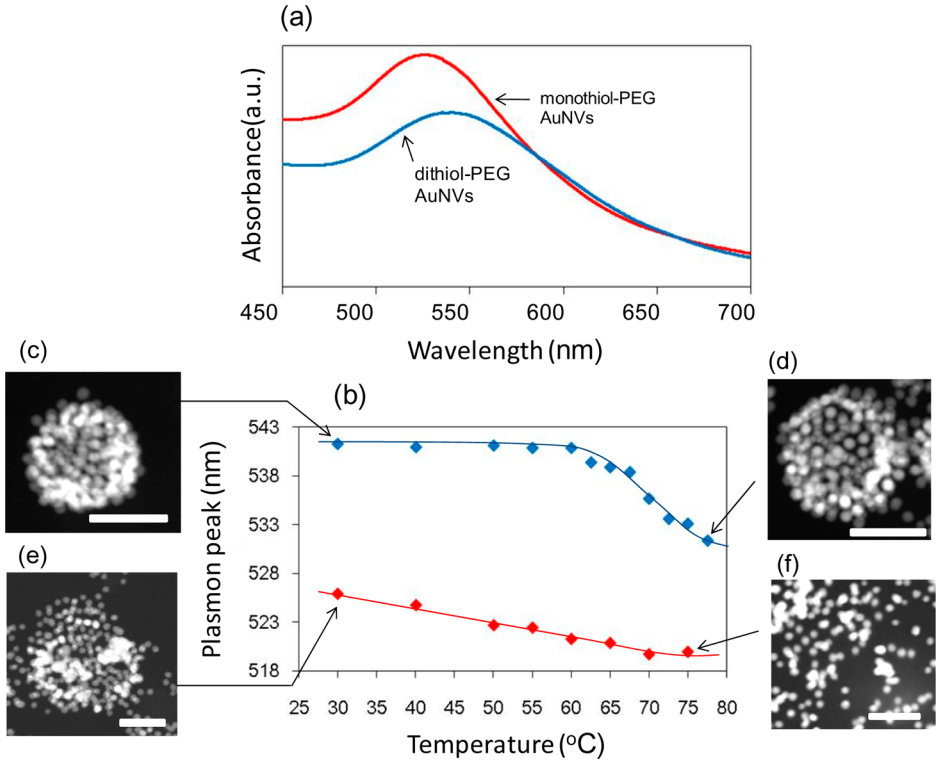

Figure 3. (a) Absorption spectra of AuNVs cross-linked with dinothiol-PEG (blue line), and modified with monothiol-PEG (red line) in water at 30 °C. The plasmon peaks are 541 nm (dithiol-PEG), and 526 nm (monothiol-PEG), respectively. (b) Plasmon peak shift of AuNVs modified with dithiol-PEG (blue dots), and monothiol-PEG (red dots) in water as a function of temperature. (c–f) STEM images of AuNVs modified with dithiol-PEG (c) before or (d) after solvent heating, or modified with monothiol-PEG (e) before or (f) after solvent heating. The scale bars are 50 nm.

the vesicles. Rhodamine dyes were not released from cross-linked AuNVs at room temperature at the tested time range (0–150 min, Figure 4a, green squares). In contrast, dye molecules were gradually released from vesicles when incubated at 70 °C (Figure 4a, blue squares).

These results revealed that cross-linked AuNVs can encapsulate dyes without leakage and release them in response to heating. As a control, dispersed AuNPs, formed by mixing dithiol-PEG with monodispersed SFL-coated AuNPs in methanol (STEM image is shown in Figure S7 in the Supporting Information), were used to evaluate the level of nonspecific adsorption of dyes on the nanoparticles (Figure 4a, red squares). Dispersed AuNPs were mixed with dyes following the same preparation scheme as that used for the cross-linked AuNVs. A much smaller amount of dyes (less than 3%) was released from the dispersed AuNPs compared to cross-linked AuNVs, which indicates that the AuNVs encapsulate dye molecules within their inner spaces. These data showed that the encapsulated dyes could be released from cross-linked AuNVs based on the heat-triggered closed-to-open change in their structure.

Dye release triggered by light-irradiation was next examined. Cross-linked AuNVs loaded with dye molecules were irradiated by diode laser (532 nm, 250 mW) to excite efficiently the AuNV plasmon bands (λ_{max} = 541 nm). Figure 4b shows the time-course of dye release as a function of irradiation time. Dye molecules were released within 5 min after the start of irradiation and the amount released from the vesicles was identical even after longer irradiation (Figure 4b, black squares), meaning that all dye molecules were released within 5 min. This release speed was much faster than that achieved by solvent heating at 70 °C in which the release were not completed even after incubation for 45 min, as shown in Figure 3b, blue squares (identical plots in Figure 4a, blue squares). Irradiation at lower power (25 mW) showed a similar release profile to that at 250 mW, which indicates that cross-linked AuNVs are highly responsive to light (Figure 4c). Because near-infrared light (650–950 nm) can penetrate biological tissues more efficiently than visible light, near-infrared light-triggered drug release will expand the practical application of AuNVs in vivo. Irradiation of 790 nm light (250 mW) to dye-encapsulating AuNVs in water allowed the release of dyes, even though the level of release was only one-fifth that induced by visible light (532 nm) irradiation (Figure 4c).

As a control, almost no release of dye molecules from dispersed AuNPs was observed after laser irradiation (Figure 4b, red squares). When monothiol-coated AuNVs were used as capsules, the level of dye release was much smaller than that for cross-linked AuNVs (Figure 4b, white squares). The number of dye molecules encapsulated in AuNP vesicles was calculated to be 470 molecules/vesicle from the fluorescence intensity of the dye molecules released from cross-linked AuNVs after laser irradiation for 45 min. STEM images taken after laser irradiation showed cross-linked AuNVs with open interparticle nanogaps in the vesicles (see Figure S6 in the Supporting Information), which is good agreement with those taken after heating. The hydrodynamic diameter was also incresed after laser irradiation (see Table S1 in the Supporting Information).

Also, the AuNVs maintained their vesicular structure after irradiation, which indicates that the dithiol-PEG layer remained on the nanoparticles and was not burned off. This data suggests that laser irradiation is much more efficient in opening the gaps in cross-linked AuNVs than is solvent heating. On the basis of the dye release upon heating shown in Figure 4a, the local

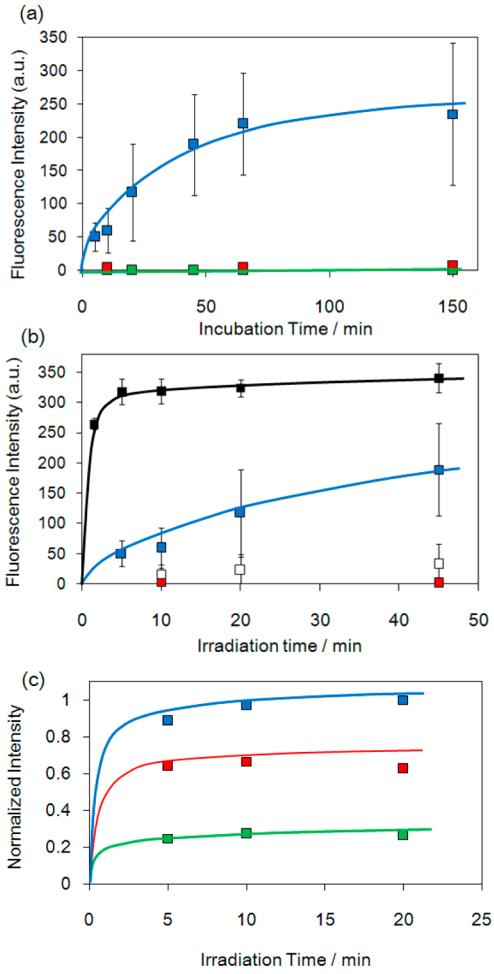

Figure 4. (a) Fluorescence intensity of Rhodamine B released from cross-linked AuNVs at 70 °C (blue squares) and 25 °C (green squares), dispersed AuNPs at 70 °C (red squares). (b) Fluorescence intensity of Rhodamine B released upon laser irradiation (532 nm, 250 mW) as a function of irradiation time. Cross-linked AuNVs with dithiol-PEG (black), AuNVs modified with monothiol-PEG (white), and dispersed AuNPs (red), respectively. For comparison, the release level upon the solvent heating of Figure 3a is shown in blue line. Errors represent the standard deviation for three replicates. (c) Normalized fluorescence intensity of Rhodamine B released upon 532 nm laser irradiation at 250 mW (blue dots) or 25 mW (red dots), and NIR-laser irradiation (790 nm) at 250 mW (green dots) as a function of irradiation time.

temperature between the AuNPs during laser-irradiation is thought to be higher than 70 °C. The temperature of the solvent remained unchanged during the experimental runs and the laser irradiation of water under the same conditions but without AuNVs also did not induce any increase in temperature. These results show that the heat necessary for opening the interparticle nanogaps was provided by the very localized heating of the AuNPs by photothermal conversion of the laser electromagnetic energy. Zink et al. demonstrated the release of Rhodamine B from mesoporous silica (ca. ~50 nm thickness)-coated gold nanoparticles (20 nm in diameter).[47] They estimated the temperature of the shell surface upon laser irradiation (514 nm, 100 mW) reached 60 °C. Because the temperature around the AuNPs is inversely proportional to the distance from the nanoparticle center,[48,49] the surface of the AuNPs is expected to be more than 100 °C. This higher temperature increases the Brownian motion of the AuNPs and/or the conformational change in cross-linking PEGs, leading to the efficient release of the encapsulated dyes. The release level of dyes from AuNVs at 95 °C was two times larger than that at 70 °C (see Figure S8 in the Supporting Information). However, the release level at 95 °C for is still one-third of that released by laser irradiation. This suggests that the local heating by the laser irradiation enhance the diffusion of encapsulated dyes via thermophoresis.[50]

Finally, we tested the light-triggered release of doxorubicin (DOX), a known anticancer drug, from cross-linked AuNVs. Cross-linked AuNVs were incubated with HeLa cells for 2 h in a culture medium, and cells were washed with phosphate-buffered saline (PBS). The number of AuNPs in a cell was calculated by inductively coupled plasma emission spectrometry (ICPES). Cross-linked AuNVs showed twice the level of cellular uptake compared with that of dispersed AuNPs (same surface chemistry) (Figure 5a). This result indicates that cross-linked AuNVs can be efficiently internalized into cells as their size is suitable for endocytosis.[51] Next, cross-linked AuNVs were mixed with DOX at 62.5 °C and purified in the same manner as that used for the dyes. DOX-encapsulated AuNVs (DOX-AuNVs) were incubated with HeLa cells for 2 h in a culture medium and cells were rinsed with PBS. The cells were irradiated by a diode laser (532 nm, 250 mW) for 5 min in the culture medium, incubated for 2 h and the cell death ratio was analyzed by counting the number of dead cells after staining with trypan blue (Figure 5b–f). The ratio of dead cells after treatment with DOX-AuNVs was markedly increased after laser irradiation; however, without laser irradiation, DOX-AuNV treatment did not affect cell viability. This means that laser irradiation promotes the release of DOX in cells, causing their drug actions. Even without staining with trypan blue, cell death induced by the laser-triggered DOX release was confirmed by characteristic changes in cell morphology (see Figure S10 in the Supporting Information). As a control, cross-linked AuNVs alone did not induce any damage to cells within tested time scale. When HeLa cells were incubated with or without cross-linked AuNVs and later exposed to the laser, the ratio of dead cells was significantly smaller than that after DOX-AuNV treatment (by Student's independent t-test, $p < 0.05$), supporting the notion that the reduced cell viability was not due to the AuNP-mediated hyperthermic effect (photothermal heating). This photothermal method might not be applicable to thermo-sensitive drugs, such as proteins. However, in this study, we demonstrated that, at least, DOXs were useful for light-triggered release. To the best of our knowledge, this is the first study to demonstrate that AuNVs can act as a drug carrier enabling the light-triggered release of drugs in cells.

4. CONCLUSION

In conclusion, AuNP vesicles cross-linked with dithiol-PEG functioned as novel nanocarriers that released encapsulated molecules upon light irradiation. Cross-linking of each nanoparticle on the surface of the AuNP vesicles with dithiol PEG made the vesicles more robust so that the vesicular structures were stable in water. We demonstrated that encapsulated dyes were released much more rapidly from the vesicles upon laser irradiation than upon solvent heating. The sub-100 nm size also contributed to the efficient cellular uptake compared with that of dispersed AuNPs. The drug delivery of DOX into cells and its light-triggered release were proved using cross-linked AuNVs. Our current system using a 532 nm laser

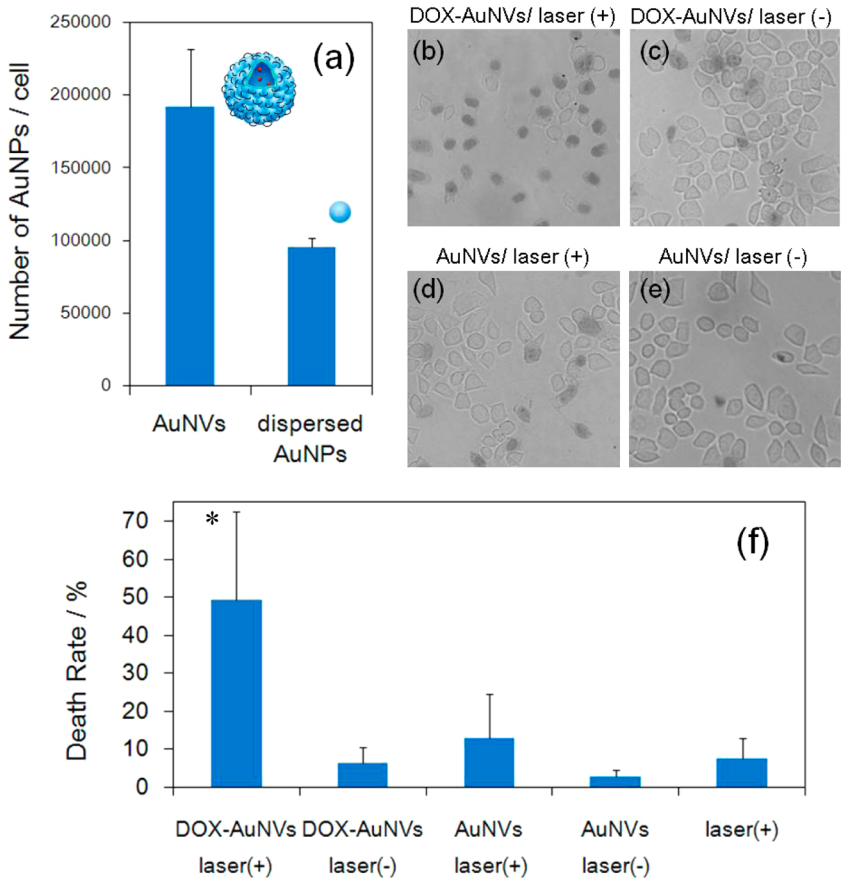

Figure 5. (a) Cellular uptake of cross-linked AuNVs (left) and dispersed AuNPs (right) per cell as determined by ICPES. The *y*-axis indicates the number of gold nanoparticles in a cell. Errors represent the standard deviation for three independent experiments. (b–e) Bright-field images of HeLa cells stained with trypan blue. HeLa cells treated with cross-linked AuNVs containing DOX were (b) irradiated by laser or (c) not. HeLa cells treated with cross-linked AuNVs alone were (d) irradiated by laser or (e) not. (f) HeLa cell death rate of the above groups and cells irradiated by laser (laser(+)). The rates were obtained by counting the cells stained blue. Errors represent the standard deviation for three independent experiments. Significant difference: $*p < 0.05$ vs AuNVs laser (+).

would open the possibility of using AuNVs as a DDS carrier in combination with optical fiber techniques for localized therapy. We are currently exploring the applicability of nanorod-based AuNVs for external beam therapy using near-infrared lasers.

■ ASSOCIATED CONTENT

Supporting Information

Supporting figures. This material is available free of charge via the Internet at http://pubs.acs.org.

■ AUTHOR INFORMATION

Corresponding Author

***Corresponding Author** E-mail: kniikura@poly.es.hokudai.ac.jp.

Notes

The authors declare no competing financial interest.

■ ACKNOWLEDGMENTS

This work was supported by JST-CREST and KAKENHI 22655050: Grant-in-Aid for challenging Exploratory Research. A part of this work was conducted at Hokkaido Innovation through Nanotechnology Support (HINTS), supported by "Nanotechnology Network JAPAN" Program of the Ministry of Education, Culture, Sports, Science and Technology (MEXT), Japan.

■ REFERENCES

(1) Niikura, K.; Iyo, N.; Higuchi, T.; Nishio, T.; Jinnai, H.; Fujitani, N.; Ijiro, K. *J. Am. Chem. Soc.* **2012**, *134*, 7632–7635.
(2) Soussan, E.; Cassel, S.; Blanzat, M.; Rico-Lattes, I. *Angew. Chem., Int. Ed.* **2009**, *48*, 274–288.
(3) Guo, X.; Szoka, F. C. *Acc. Chem. Res.* **2003**, *36*, 335–341.
(4) Nakamura, T.; Akita, H.; Yamada, Y.; Hatakeyama, H.; Harashima, H. *Acc. Chem. Res.* **2012**, *45*, 1113–1121.
(5) Becker, A. L.; Johnston, A. P. R.; Caruso, F. *Small* **2010**, *6*, 1836–1852.
(6) Peyratout, C. S.; Dähne, L. *Angew. Chem., Int. Ed.* **2004**, *43*, 3762–3783.
(7) Jianhao, B.; Sebastian, B.; Yein, T. S.; Dieter, T. *ACS Appl. Mater. Interfaces* **2011**, *3*, 1665–1674.
(8) Ohtake, N.; Niikura, K.; Suzuki, T.; Nagakawa, K.; Mikuni, S.; Matsuo, Y.; Kinjo, M.; Sawa, H.; Ijiro, K. *ChemBioChem* **2010**, *11*, 959–962.
(9) Niikura, K.; Sugimura, N.; Musashi, Y.; Mikuni, S.; Matsuo, Y.; Kobayashi, S.; Nagakawa, K.; Takahara, S.; Takeuchi, C.; Sawa, H.; Kinjo, M.; Ijiro, K. *Mol. BioSyst.* **2013**, *9*, 501–507.
(10) Esser-Kahn, A. P.; Odom, S. A.; Sottos, N. R.; White, S. R.; Moore, J. S. *Macromolecules* **2011**, *44*, 5539–5553.
(11) Moghimi, S. M.; Hunter, A. C.; Murray, J. C. *Pharmacol. Rev.* **2001**, *53*, 283–318.
(12) Cabral, H.; Matsumoto, Y.; Mizuno, K.; Chen, Q.; Murakami, M.; Kimura, M.; Terada, Y.; Kano, M. R.; Miyazono, K.; Uesaka, M.; Nishiyama, N.; Kataoka, K. *Nat. Nanotechnol.* **2011**, *6*, 815–823.

(13) El-Sayed, I. H.; Huang, X.; El-Sayed, M. A. *Cancer Lett.* **2006**, *239*, 129−135.
(14) Huang, X.; El-Sayed, I. H.; Qian, W.; El-Sayed, M. a *J. Am. Chem. Soc.* **2006**, *128*, 2115−2120.
(15) Ghosh, S. K.; Pal, T. *Chem. Rev.* **2007**, *107*, 4797−47862.
(16) Qin, Z.; Bischof, J. C. *Chem. Soc. Rev.* **2012**, *41*, 1191−217.
(17) Zhang, J. Z. *J. Phys. Chem. Lett.* **2010**, *1*, 686−695.
(18) Kawano, T.; Niidome, Y.; Mori, T.; Katayama, Y.; Niidome, T. *Bioconjugate Chem.* **2009**, *20*, 209−212.
(19) Paasonen, L.; Laaksonen, T.; Johans, C.; Yliperttula, M.; Kontturi, K.; Urtti, A. *J. Controlled Release* **2007**, *122*, 86−93.
(20) Angelatos, A. S.; Radt, B.; Caruso, F. *J. Phys. Chem. B* **2005**, *109*, 3071−3076.
(21) Radt, B.; Smith, T. a.; Caruso, F. *Adv. Mater.* **2004**, *16*, 2184−2189.
(22) Zhang, Z.; Wang, L.; Wang, J.; Jiang, X.; Li, X.; Hu, Z.; Ji, Y.; Wu, X.; Chen, C. *Adv. Mater.* **2012**, *24*, 1418−1423.
(23) Wang, Y.; Li, B.; Zhang, L.; Song, H.; Zhang, L. *ACS Appl. Mater. Interfaces* **2013**, *5*, 11−15.
(24) Bikram, M.; Gobin, A. M.; Whitmire, R. E.; West, J. L. *J. Controlled Release* **2007**, *123*, 219−227.
(25) Nishio, T.; Niikura, K.; Matsuo, Y.; Ijiro, K. *Chem. Commun.* **2010**, *46*, 8977−8979.
(26) Sekiguchi, S.; Niikura, K.; Iyo, N.; Matsuo, Y.; Eguchi, A.; Nakabayashi, T. *ACS Appl. Mater. Interfaces* **2011**, 4169−4173.
(27) Dinsmore, A. D.; Hsu, M. F.; Nikolaides, M. G.; Marquez, M.; Bausch, A R.; Weitz, D. A. *Science* **2002**, *298*, 1006−1009.
(28) Patra, D.; Sanyal, A.; Rotello, V. M. *Chem. Asian J.* **2010**, *5*, 2442−2453.
(29) He, J.; Liu, Y.; Babu, T.; Wei, Z.; Nie, Z. *J. Am. Chem. Soc.* **2012**, *134*, 11342−11345.
(30) Nie, Z.; Fava, D.; Kumacheva, E.; Zou, S.; Walker, G. C.; Rubinstein, M. *Nat. Mater.* **2007**, *6*, 609−614.
(31) Nikolic, M. S.; Olsson, C.; Salcher, A.; Kornowski, A.; Rank, A.; Schubert, R.; Frömsdorf, A.; Weller, H.; Förster, S. *Angew. Chem., Int. Ed.* **2009**, *48*, 2752−2754.
(32) Cha, J. N.; Birkedal, H.; Euliss, L. E.; Bartl, M. H.; Wong, M. S.; Deming, T. J.; Stucky, G. D. *J. Am. Chem. Soc.* **2003**, *125*, 8285−8289.
(33) Song, J.; Cheng, L.; Liu, A.; Yin, J.; Kuang, M.; Duan, H. *J. Am. Chem. Soc.* **2011**, *133*, 10760−10763.
(34) An, X.; Zhang, F.; Zhu, Y.; Shen, W. *Chem. Commun.* **2010**, *46*, 7202−7204.
(35) Yavuz, M. S.; Cheng, Y.; Chen, J.; Cobley, C. M.; Zhang, Q.; Rycenga, M.; Xie, J.; Kim, C.; Song, K. H.; Schwartz, A. G.; Wang, L. V; Xia, Y. *Nat. Mater.* **2009**, *8*, 935−939.
(36) Yang, X.-C.; Samanta, B.; Agasti, S. S.; Jeong, Y.; Zhu, Z.-J.; Rana, S.; Miranda, O. R.; Rotello, V. M. *Angew. Chem., Int. Ed.* **2011**, *50*, 477−481.
(37) Song, J.; Zhou, J.; Duan, H. *J. Am. Chem. Soc.* **2012**, *134*, 13458−13469.
(38) He, J.; Zhang, P.; Babu, T.; Liu, Y.; Gong, J.; Nie, Z. *Chem. Commun.* **2013**, *49*, 576−578.
(39) He, J.; Wei, Z.; Wang, L.; Tomova, Z.; Babu, T.; Wang, C.; Han, X.; Fourkas, J. T.; Nie, Z. *Angew. Chem., Int. Ed.* **2013**, *52*, 1−7.
(40) Trabelsi, S.; Zhang, S.; Zhang, Z.; Lee, T. R.; Schwartz, D. K. *Soft Matter* **2009**, *5*, 750−758.
(41) Malone, S. M.; Trabelsi, S.; Zhang, S.; Lee, T. R.; Schwartz, D. K. *J. Phys. Chem. B* **2010**, *114*, 8616−8620.
(42) Ishikawa, Y.; Kuwahara, H.; Kunitake, T. *J. Am. Chem. Soc.* **1994**, *116*, 5579−5591.
(43) Nagahori, N.; Ab, M.; Nishimura, S.-I. *Biochemistry* **2009**, *48*, 583−594.
(44) Bjorling, M.; Karlstriim, G.; Linse, P. *J. Phys. Chem.* **1991**, *95*, 6706−6709.
(45) Lutz, J.-F. J. *Polym. Sci. Part A: Polym. Chem.* **2008**, *46*, 3459−3470.
(46) Jain, P. K.; El-Sayed, M. A. *J. Phys. Chem. C* **2008**, *112*, 4954−4960.
(47) Croissant, J.; Zink, J. I. *J. Am. Chem. Soc.* **2012**, *134*, 7628−7631.
(48) Kyrsting, A.; Bendix, P. M.; Stamou, D. G.; Oddershede, L. B. *Nano Lett.* **2011**, *11*, 888−892.
(49) Bendix, P. M.; Reihani, S. N. S.; Oddershede, L. B. *ACS Nano* **2010**, *4*, 2256−2262.
(50) Duhr, S.; Braun, D. *Proc Natl. Acad. Sci. U.S.A.* **2006**, *103*, 19678−19682.
(51) Chithrani, B. D.; Chan, W. C. W. *Nano Lett.* **2007**, *7*, 1542−1550.